4 A Deep Survey for Extremely Metal-Poor Halo Stars

4.1 Introduction

A question that has been asked by astronomers for a long time is whether so-called population III (Pop. III) stars exist. Bond (1981) "roughly" defines them "as stars with [Fe/H] < -3". Of *such* stars, ~ 100 are known today (Beers 1999), but today other definitions of Pop. III are used. Cayrel (1996) defines them as stars "with strictly the chemical composition left by the Big Bang", and Beers (2000*b*), for practical reasons, adds the criterion that such stars should have "a measurable atmospheric abundance of [Fe/H] < -6". Cayrel (1996) estimates the number of Pop. III stars expected to be discovered within the survey of Beers et al. (1992), when completed, to 1.8. However, in estimations like this it is assumed that first generation of stars includes low-mass stars. The mass spectrum of the first generation of is not known, and actually *no* Pop. III star has yet been found (Beers 1999). On the other hand, the absence of Pop. III stars in current samples of metal-poor stars is hardly significant: Today, only 18 stars of [Fe/H] < -3.5 are known (Beers 1999), of which only 5 have their abundances confirmed by high resolution spectroscopy (Beers 2000, priv. comm.). The discovery of a Pop. III star would offer the possibility to study primordial matter, whereas their *quantified* absence would put important constraints to models of the formation of the first generation of stars in our Galaxy, so that either case is interesting in itself.

The chemical compositions of the *second* generation of stars, i.e. extremely metal-poor halo stars (hereafter shortly referred to as MPHS) of [Fe/H] < -2.5, provide detailed information on the early chemical evolution of the Galaxy, and on nucleosynthesis in the first generation of stars. There is evidence that the abundance patterns seen in MPHS can be attributed to individual supernovae of type II (e.g., Shigeyama & Tsujimoto 1998; Tsujimoto et al. 2000).

MPHS also have cosmological applications. The oldest stars provide a lower limit for the age of the Universe, yielding constraints for the cosmological parameters. How can we find the oldest stars? Models of Galactic chemical evolution predict that heavy element abundances, e.g. [Fe/H], are no good age indicators, because mixing of nucleosynthesis products of SN II into the interstellar gas is very inefficient (see e.g. Beers et al. 2000*b*). This means that at given metallicity, there is likely a large scatter of stellar ages, and *some* metal-poor stars can be rather young. However, with increasing time, the interstellar gas is more and more enriched by the nucleosynthesis products of SN II (and later, SN I), so that there is higher chance for young stars to be metal-rich than to be metal-poor. Conversely, if we look at very metal-poor stars, we will find more old stars among them than in a sample of metal-rich stars.

Individual ages of stars can best be measured by two methods: by nucleocosmochronology, and with individual fitting of evolutionary paths. The former is feasible for stars showing an r-process abundance pattern, and having spectra with detectable Thorium (and optionally, Uranium) lines. Today, only two such stars are known: HD 115444 and CS 22892-052 (Cowan et al. 1999). Ages can be derived using the abundance ratios [Th/Eu] and [Th/U]. However, the accuracy achievable with this method, when including *theoretical* uncertainties, is ± 4 Gyrs only (Cowan et al. 1999). A higher accuracy (± 2 Gyrs) can be reached by fitting of individual evolutionary tracks to accurate stellar parameters $T_{\rm eff}$, $\log g$, [Fe/H] and [α/H] (Bernkopf & Gehren 1999, priv. comm; see also Fuhrmann 1999).

If individual ages are obtained for a large sample of MPHS, this would offer the opportunity to study the chemical evolution of the Galaxy *directly* as a function of time. Up to now, one has to use secondary age indicators, like [Fe/H]. As already argued above, such age indicators are likely not valid for population II, due to inhomogeneous mixing of the interstellar matter.

~ 100 stars of [Fe/H] < -3.0 might sound like a large sample. However, in practice one often

has to select suitable subsamples of objects. For example, when studying Lithium abundances, it is necessary to restrict the sample to a narrow temperature range, in order to avoid influences of temperature dependent effects, like depletion; for other studies, one wants to select subsamples by kinematic properties. Moreover, the fraction of binaries among the most metal-poor stars is unclear. Abundance analysis of single-lined binaries may be complicated, or even impossible. Last but not least, any *new* questions are sure to arise from the first-pass 8 m-class telescope follow-ups (see Beers 2000*a*), which likely can only be answered by larger samples of extremely metal-poor stars.

For all these reasons, it is desirable to enlarge the survey volume for extremely metal-poor stars *now*, which currently can be only accomplished by the HES (for a review of ongoing surveys for metal-poor stars see Beers 2000*b*). Our specific aims are:

(a) Providing a *quantitative* answer to the question of the existence of Pop. III. This is possible in the HES, since the survey volume can be enlarged with the HES, making the absence of Pop. III stars more significant in case no such object will be found. In contrast to the HK survey, in the HES the selection function of MPHS can be determined by simulations, so that we would be able to quantify the (possible) absence of Pop. III stars.

(b) Enlarging the sample of stars with [Fe/H] < -3.0.

(c) Finding more stars with r-process abundance patterns and detectable Th lines, like CS 22892-052, for age determination.

In order to elucidate what the advantages of the HES compared to the so-called HK survey of Beers et al. (1992) are, we give a detailed comparison of both surveys in the next section. An overview can be found in Tab. 7.

		HK survey	HES
Telescope	north	0.6 m Burrell Schmidt	—
	south	0.6 m Curtis Schmidt	1 m ESO Schmidt
Magnitude range		$11.0 \lesssim B \lesssim 15.5$	$14.0 \lesssim B \lesssim 17$
Widened?		yes	no
Area	north	$2800\,\square^\circ$	—
	south	$4100\,\square^\circ$	$7600\,\square^\circ$
Objective prism		4°	4°
Dispersion		180 Å/mm	450 Å/mm
Spectral resolution		~ 5 Å	~ 10 Å at Ca K
Photographic emulsion		103a-O/IIa-O	IIIa-J
Filter?		interference/Ca H+K	no
Wavelength range		$3875\,\text{Å} < \lambda < 4025\,\text{Å}$	$3200\,\text{Å} < \lambda \lesssim 5200\,\text{Å}$
Candidate selection		visual inspection	automated

Table 7: Comparison of the HK survey and the HES.

4.2 Comparison of HES and HK survey

The HK survey was started in 1978 by G. Preston and S. Shectman of the Carnegie Observatories of Washington. It is based on objective prism plates taken with the 60 cm Burrell Schmidt (northern

hemisphere) and Curtis Schmidt (southern hemisphere) telescopes. As in the HES, each photographic plate covers a nominal area of $5^\circ \times 5^\circ$ of the sky. The name "HK survey" is used because in addition to a 4° objective prism (leading to a seeing-limited spectral resolution of ~ 5 Å), an interference filter was mounted on the plate holder to limit the wavelength coverage to ~ 150 Å centered on the Ca H+K resonance lines, effectively reducing the sky background level so that long exposures (typically 90 minutes) could be obtained. In 1983 Beers joined the team, and later expanded the survey with an additional 240 plates in the southern and northern hemispheres. By 1992, 308 acceptable-quality plates were obtained (275 of which are unique). Note that due to the small spectral range of the HK survey, overlapping spectra are much less of a problem than in the HES. Further extension of the HK survey area was prevented by the shortage of photographic plates with 103a-O and IIa-O emulsions. HES areas in common with the HK survey are shown in Fig. 19.

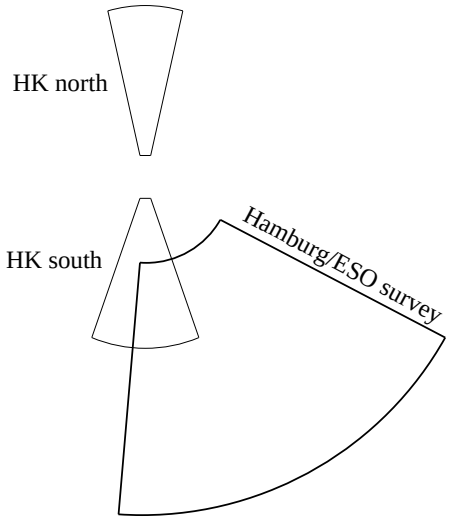

Figure 18: Comparison of HES and HK survey volumes.

The use of a larger telescope, and a 2 times lower resolution of the HES compared to the HK survey, results in a limiting magnitude of about $B = 17.5$. However, we restricted the selection of metal-poor candidate stars in the HES to $S/N > 10$, because it was found that below this S/N level it is extremely difficult to select objects by the absence of individual spectral lines, i.e., the Ca K line in case of metal-poor stars. In result, the faintest low-metallicity candidates in the HES sample reach $B \sim 17$, about 1.5 magnitudes deeper than the HK survey. Spectra of bright objects close to saturation were also excluded from the search for metal-poor stars, because at high illumination, when the characteristic curve of the photographic emulsion gets flatter (at the "shoulder"), the contrast between continuum and spectral lines gets weaker, and apparently *all* stars have weak lines. The saturation threshold chosen in the HES corresponds to $B \sim 14.0$. Taking the common area of both surveys and their magnitude ranges into account, the HES can increase the total survey volume for metal-poor stars by a factor of 8 compared to the HK survey alone (see also Fig. 18).

Candidate selection in the HK survey was done by visual inspection of the widened objective-prism spectra with a binocular $10\times$ microscope. Each plate was inspected twice, with a time lag of a month or more between the two inspections. Candidates were identified on the basis of the observed strengths of their Ca lines, and grouped into rough categories based on this criteria (e.g., possibly metal-poor, metal-poor, and extremely metal-poor). Positions of the candidates were noted on the plates, and coordinates for each candidate were measured later (individually, with Grant machines). In this process, a total of about 10 000 metal-poor candidates was selected (roughly half of which have had medium-resolution

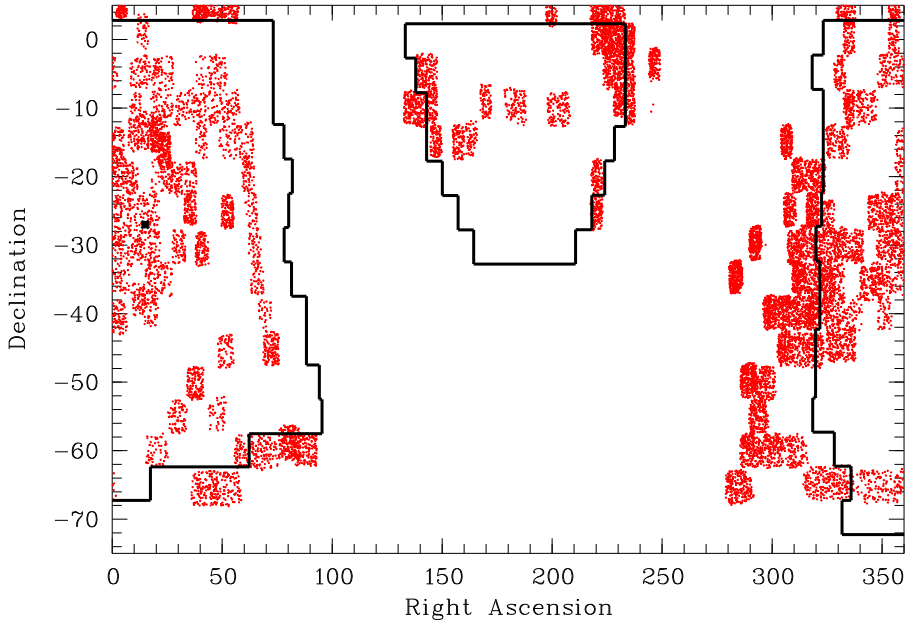

Figure 19: Comparison of HES area (framed) with HK survey area. Dots denote all HK survey candidates in the southern hemisphere.

follow-up spectroscopy obtained to date).

One major advantage of the HES is that the candidate selection is done *automatically*, with *quantifiable* selection criteria. We will show in Sect. 4.5 that although the spectral resolution of the HES is $2\times$ lower than in the HK survey, candidate selection in the HES is up to 3–$7\times$ more efficient than in the HK.

4.3 Candidate Selection in the HES

For the present, we have restricted the selection of metal-poor stars in the HES to the color range $0.3 < B-V < 0.5$, because we decided to focus at first on main-sequence turnoff stars. One of the most interesting applications for these stars is individual age determination based on precise stellar parameters obtained spectroscopically from high-resolution, high S/N observations. However, with a few adaptions the selection procedures described below can easily also be used for cooler stars.

Candidate selection in the HES has been done by two techniques: The Ca K index method and via automatic classification. An alternative, third approach is to determine stellar parameters directly from HES spectra by calibrating spectral features against a learning sample.

4.3.1 The Ca K Index Method

In the Ca K index method, stars are selected when their Ca K line is significantly weaker than "normal." "Normality" is determined by a least squares fit of a 2nd order polynomial to the Ca K index relative to the parameter `x_hpp2`. At the time this selection technique was used, it was not yet clear that the use of `dx_hpp2` instead of `x_hpp2` leads to a more accurate $B-V$ colour estimation.

A first set of candidates found with this techniques has been observed in spectroscopic follow-up campaigns at the ESO NTT. In Tab. 24 in Appendix A we list the stars found in this effort. Unfortu-

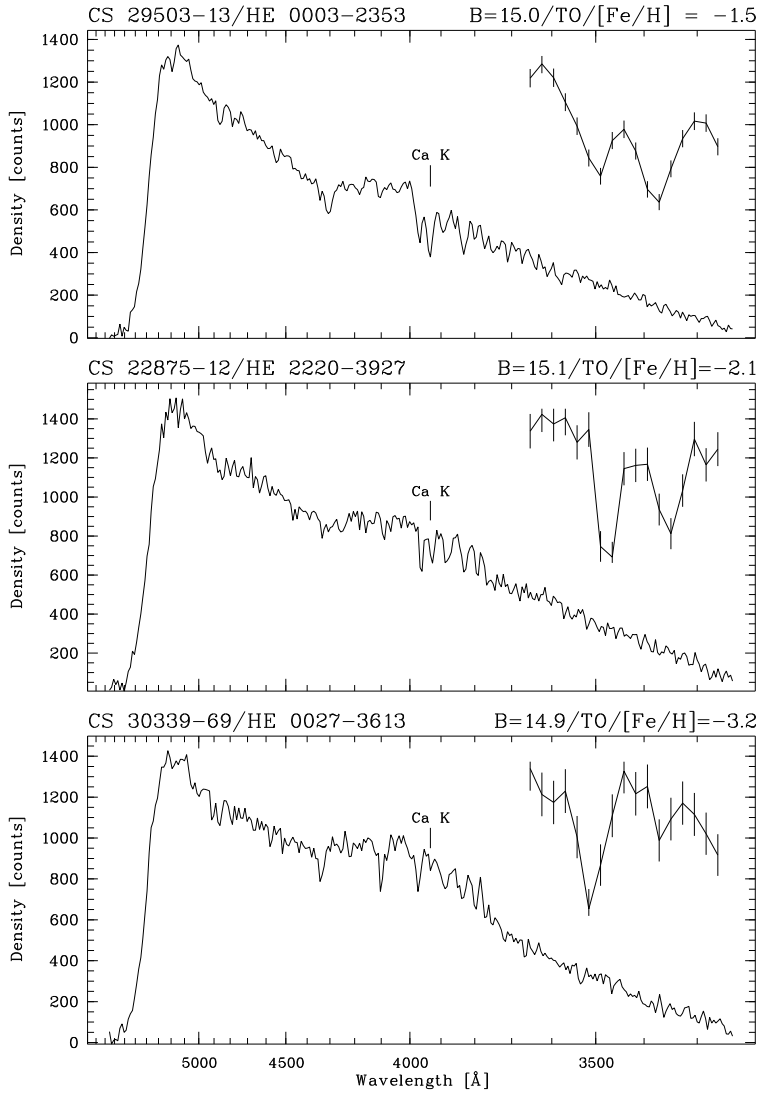

Figure 20: Examples of HES spectra of metal-poor turnoff stars discovered in the HK survey. In the upper right corner of each plot a blow-up of the Ca H+K region is shown, with an over-plot of the pixel-wise $1\,\sigma$ noise. Note that the detection of Ca K in the lower spectrum is not significant. Metal abundances are on the re-calibrated HK survey scale of Beers et al. (1999).

nately, due to bad weather, and continued technical problems, it was not yet possible to evaluate the quality of the Ca K index selection method. A set of ~ 40 spectra have been obtained at the McDonald 2.7 m and CTIO 4 m telescopes recently by T. Beers, and will be analyzed as soon as the data has been reduced.

4.3.2 Automatic Spectral Classification

For automatic classification of metal-poor stars, we use a learning sample consisting of 45 classes defined by the following grid points:

$$T_{\rm eff} \;=\; 5800\,{\rm K}, 6400\,{\rm K}, 6800\,{\rm K}$$

$$\begin{aligned} \log g &= 2.2, 3.8, 4.6 \\ [\mathrm{Fe/H}] &= -0.9, -1.5, -2.1, -2.7, -3.3 \end{aligned}$$

The learning sample has again been constructed by converting model spectra to simulated objective-prism spectra, as described in Sect. 3.1.

A set 11 of features was selected as a basis for searching the best combination: the strengths of Ca K, measured by the absorption line fit algorithm, and by an index method; the sum of the equivalent widths of Hβ, Hγ and Hδ; the Strömgren coefficient c_1, two continuum principal components, and the half-power points `x_hpp1` and `x_hpp2`. Half power points themselves instead of distances to the cutoff values have to be used since the latter cannot be determined for simulated spectra. Apart from these "standard features" we carried out a principal component analysis of a set of 165 000 simulated spectra, and used the first 3 principal components, accounting for 90.5 % of the variance in the set of simulated spectra, as additional features (see Fig. 21 for the Eigenvectors).

By evaluating all $2^{11} - 1 = 2047$ possible feature combinations at each S/N step by the "leaving one out" method, we identified the feature combinations leading to the lowest number of misclassifications (see Tab. 8). In order to explore the classification accuracy, we used Bayes' rule instead of the minimum cost rule for classification, and assumed equal prior probabilities $P(\Omega_j)$ for each class, because otherwise the estimation of the classification accuracy would be distorted.

Feature	S/N					
	30	25	20	15	10	5
`all3934eqw`	1	1	1	1	1	1
`CaKindex`	1	1	1	1	0	0
`cklcomp_1`	0	0	1	0	0	0
`cklcomp_2`	0	1	0	0	0	0
`balmsum`	1	1	1	1	0	1
`x_hpp1`	1	1	1	0	0	0
`x_hpp2`	1	1	1	1	1	1
`sklcomp_1`	1	1	1	1	1	1
`sklcomp_2`	1	1	1	1	1	1
`sklcomp_3`	1	1	1	1	1	1
`strc1`	0	0	0	1	0	0
$N =$	8	8	9	8	5	6

Table 8: Best feature combinations for Bayes classification of metal-poor stars in the colour range $0.3 < B-V < 0.5$.

The formal classification errors determined are $\sigma_{T_{\rm eff}} < 160$ K, $\sigma_{\log g} < 0.34$ dex $\sigma_{\rm [Fe/H]} < 0.71$; for $S/N > 15$, i.e. for 2/3 of the HES spectra, the errors are $\sigma_{T_{\rm eff}} < 65$ K, $\sigma_{\log g} < 0.06$ dex $\sigma_{\rm [Fe/H]} < 0.68$. That is, the error estimates for $T_{\rm eff}$ and $\log g$ *are not to be believed*. First of all, our grid of model atmospheres is not dense enough to detect such low errors. Moreover, such accuracies are not even achievable with high-resolution, high S/N spectra. Apart from the grid being too wide, we suspect that there is a systematic difference between our learning (and test) sample, and sets of real spectra.

Considerable effort has been invested in making the simulated objective prism spectra as realistic as possible, and we can exclude with high confidence that the difference is due to the simulated spectra *themselves*. The most reasonable explanation for our too optimistic error estimate is the following. The

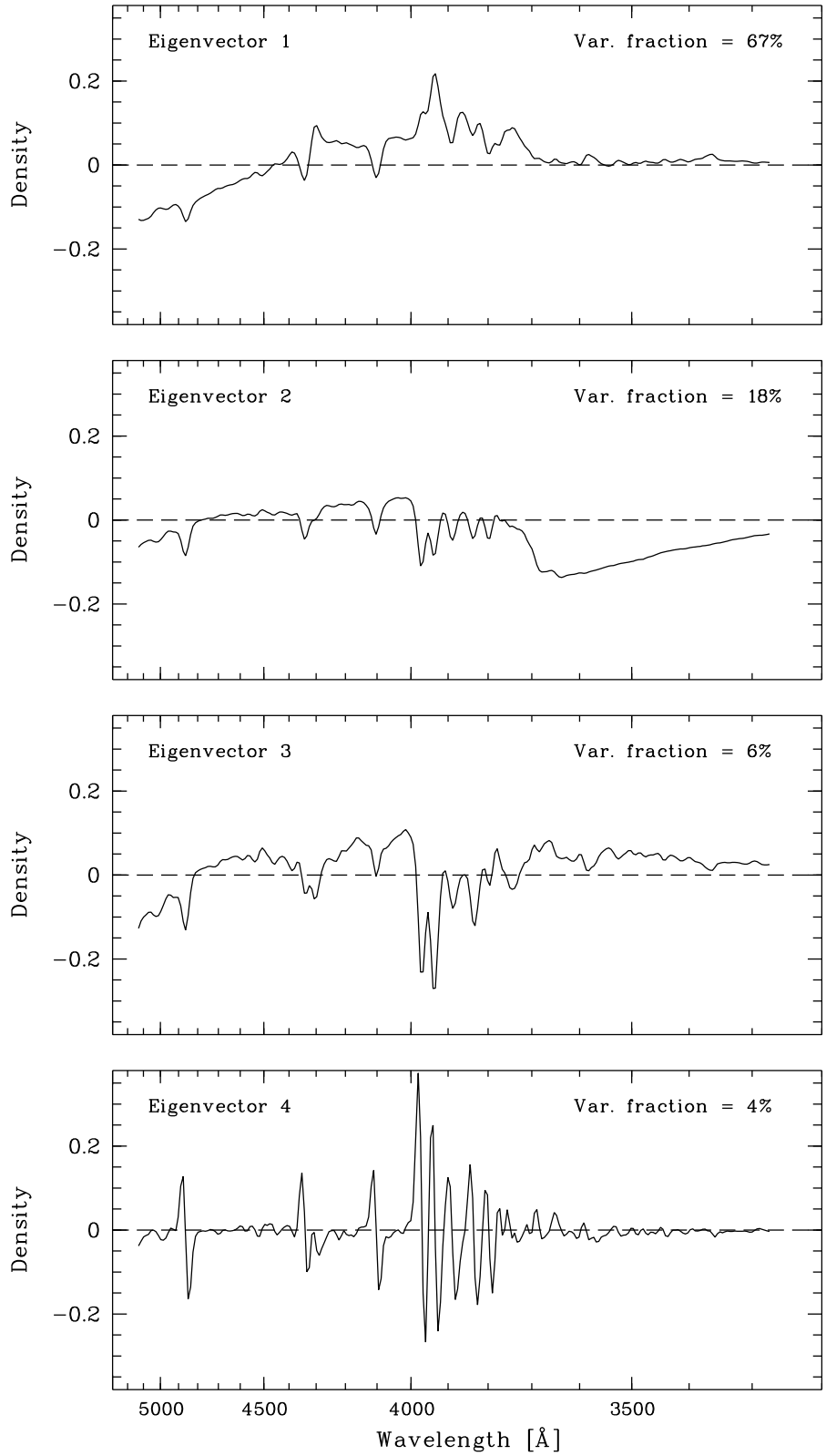

Figure 21: First four Eigenvectors of a sample of 165 000 simulated objective prism spectra for metal-poor stars. The first Eigenvector models the Balmer lines, and $B-V$; the latter is accomplished by changing the continuum slope. The second Eigenvector influences the Balmer discontinuity, the Balmer lines, and Ca H+K. In the third, Ca H+K can be seen even more prominently. The G-band of CH at $\lambda = 4300$ Å can also be seen. The forth Eigenvector mainly accounts for small shifts in the wavelength zero points.

spectra in our learning and test samples have stellar parameters belonging to a *discrete grid*, whereas in reality, the stellar parameters are distributed *continously*. A spectrum with stellar parameters between two grid points is misclassified at least with errors corresponding to (at least) half of the grid point distance, which is $\Delta T_{\rm eff} = 100\,{\rm K}$, $\Delta \log g = 0.4\,{\rm dex}$, and $\Delta[{\rm Fe/H}] = 0.15\,{\rm dex}$ (for $[{\rm Fe/H}] < -0.9$). However, spectra between grid points *do not exist* in our test samples, so that we underestimate the mean errors.

The only ways out of this trap are: (a) testing the classification with sets of real spectra, having a continuous parameter distribution; or (b), making the grid "pseudo-continuous", i.e., so fine that there is no noticeable difference between the spectra belonging to two neighboring grid points. The latter is rather resource demanding, since the number of grid points in three-dimensional parameter space raises to the third power; that is, halving the grid point distance in each dimension lets the number of grid points grow by a factor of $((2n-1)/n)^3$.

As test sample with continuous stellar parameter distribution we tried to use 262 stars from the HK survey present on HES plates, with available [Fe/H] estimate, not saturated in the HES, and in the range covered by our model spectra grid, i.e. $0.3 < B-V < 0.5$. Unfortunately, $T_{\rm eff}$ and $\log g$ are not directly determined in the HK survey, so that only our [Fe/H] estimations could be tested. However, it turned out that only 4 of the 262 objects have an $a.i. < 0.99$; that is, almost all spectra have been rejected from classification. This has likely again to be attributed to a too narrow model spectra grid.

In conclusion, the above considerations indicate that our grid of model spectra is not pseudo-continuous in $T_{\rm eff}$ and $\log g$. This partly is very good news, since it means that there *is* a noticeable difference between the spectra of two neighboring grid points; that is, we can likely classify the HES spectra with an accuracy better then $\sigma_{T_{\rm eff}} \sim 200\,{\rm K}$, and $\sigma_{\log g} \sim 0.8\,{\rm dex}$, at least at high S/N.

4.3.3 The Feature Calibration Approach

We investigated how precise $T_{\rm eff}$, $\log g$ and [Fe/H] can be determined from HES spectra directly, by calibrating HES features against a learning sample of simulated objective prism spectra. If this is possible with an acceptable accuracy, an alternative way of selecting candidates for extremely metal-poor stars would be offered.

In the first step of our investigation we carried out a parameter study to investigate which stellar features a suitable for our purpose. In the study we used a denser grid of model spectra, defined by the following grid points:

$$\begin{aligned} T_{\rm eff} &= 5600(200)6800\,{\rm K} \\ \log g &= 2.2(0.8)4.6 \\ [{\rm Fe/H}] &= -0.3, -0.9, -1.5(0.3) - 3.6 \end{aligned}$$

Each of the model spectra has been converted to 500 objective prism spectra, involving randomized spectral sensitivity curves, and smoothed with a Gaussian profile of $45\,\mu$m FWHM, corresponding to an average seeing profile width in the HES. The S/N of the simulated objective prism spectra has been decreased to $S/N = 30$ by adding Gaussian noise.

Effective Temperature Indicators Possible indicators for $T_{\rm eff}$ are `x_hpp2`, the sum of the equivalent widths of Hβ, Hγ and Hδ, determined with the feature detection algorithm described in Sect. 3.2.1, and the first spectral principal component (SPC), `sklcomp_1`.

`x_hpp2` and `sklcomp_1` are very good $T_{\rm eff}$ indicators: From Fig. 22 one can estimate that at $S/N = 30$, $T_{\rm eff}$ can be determined with an accuracy of in the order of $\pm 200\,{\rm K}$ with them. The Balmer

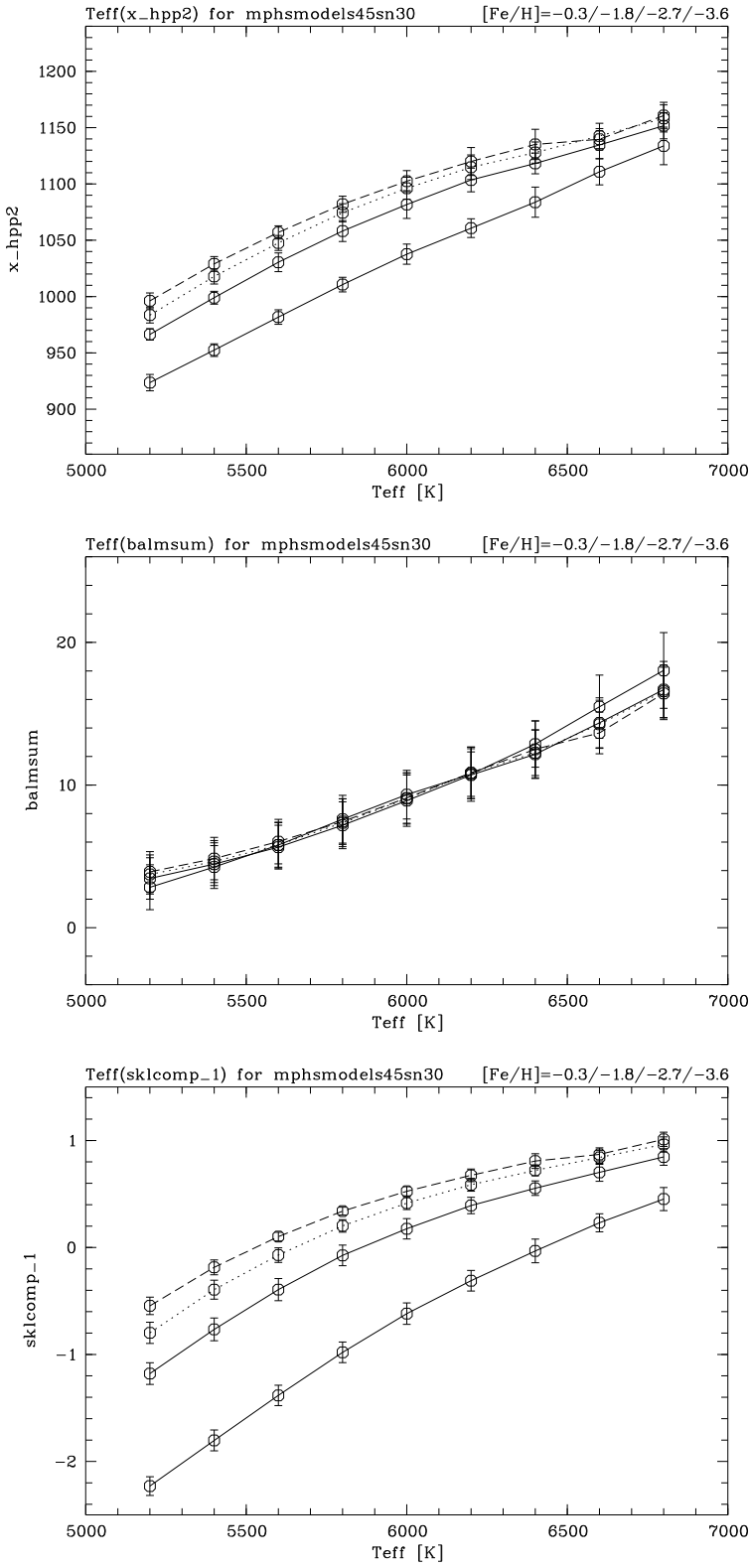

Figure 22: Investigation of possible effective temperature indicators in HES spectra.

line sum is a slightly worse indicator, leading to an accuracy of $\sim 400\,\mathrm{K}$. However, `x_hpp2` and `sklcomp_1` show a strong dependence on [Fe/H], whereas the Balmer line sum is almost completely independent of metallicity.

Gravity Indicators Strömgren c_1 is a possible gravity indicator, since it measures the strength of the Balmer jump. The 2nd SPC might also be suitable, since the corresponding Eigenvector seems to be responsible for modelling the Balmer jump. However, it turned out that c_1 is by far a better gravity indicator (see Fig. 23). Both features show a strong temperature dependence.

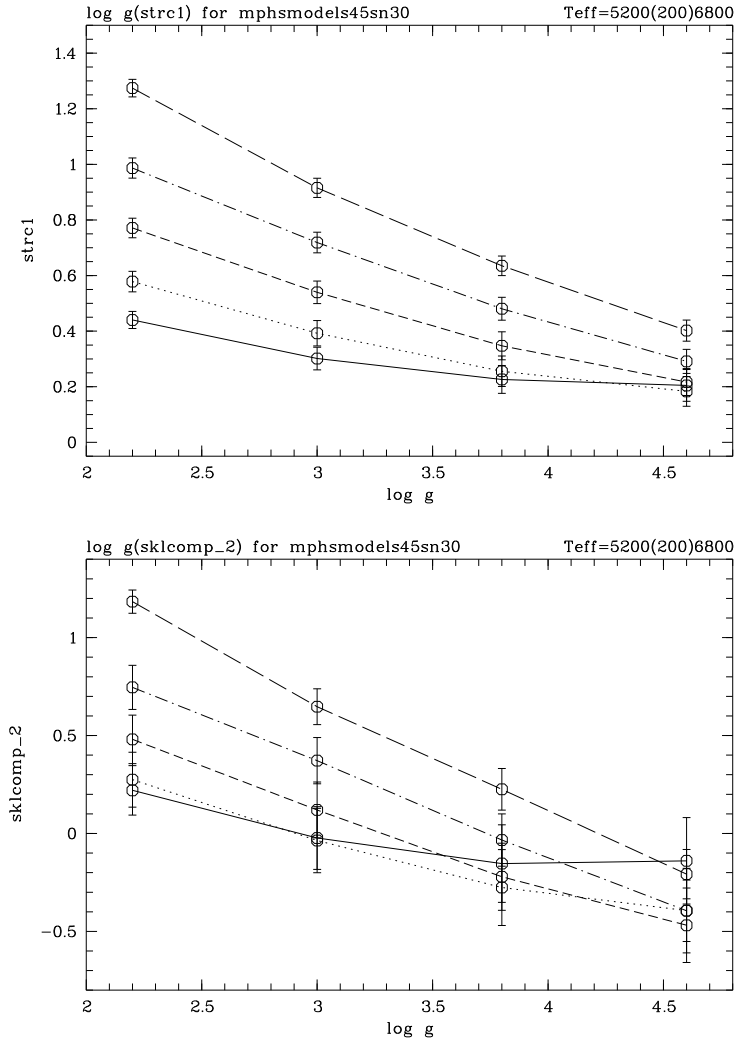

Figure 23: Investigation of possible gravity indicators in HES spectra.

Metallicity Indicators The Ca K line is the most usefull metallicity indicator, because the Ca K line is by far the strongest metal line seen in cool stars. Ca H is not suitable, since it is blended with Hε. We measure the strengths of Ca K in HES spectra with two methods: With a line fitting algorithm (yielding the feature `all3934eqw`), and with an index (`CaKindex`). The 3rd SPC contributes to modelling the Ca H+K lines, so it was investigated as well.

As is displayed in Fig. 24, the 3rd SPC shows only a weak dependence on [Fe/H]. `all3934eqw`

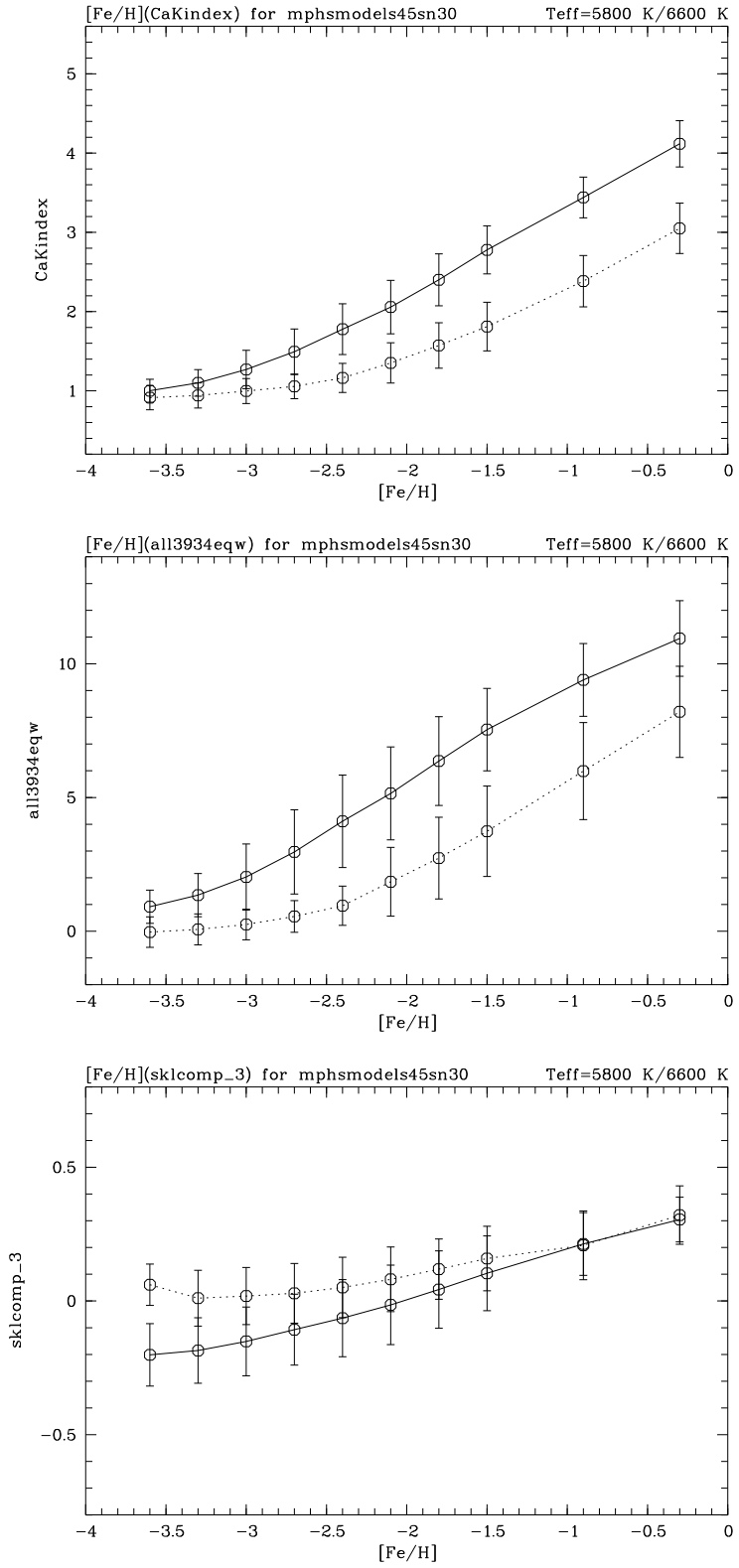

Figure 24: Investigation of possible metallicity indicators in HES spectra.

and `CaKindex` are both suitable. However, investigation of lower S/N spectra revealed that the former is less robust against noise.

Within the set of 165 000 simulated spectra available for each S/N step, we averaged the values of the features under consideration over all 500 simulatd spectra having the same spectral parameters $T_{\rm eff}$, $\log g$, [Fe/H]. To these data points, the following models were fitted with a least squares fit:

$$T_{\rm eff} = a_1 + a_2 \cdot \texttt{sklcomp\_1} + a_3 \cdot \texttt{CaKindex} + a_4 \cdot \texttt{sklcomp\_1}^2 + a_5 \cdot \texttt{CaKindex}^2 \quad (16)$$

$$T_{\rm eff} = a_1 + a_2 \cdot \texttt{balmsum} + a_3 \cdot \texttt{balmsum}^2 \quad (17)$$

$$\log g = a_1 + a_2 \cdot c_1 + a_3 \cdot \texttt{balmsum} + a_4 \cdot c_1^2 + a_5 \cdot \texttt{balmsum}^2 \quad (18)$$

$$[\text{Fe/H}] = a_1 + a_2 \cdot \texttt{CaKindex} + a_3 \cdot \texttt{sklcomp\_1} + a_4 \cdot \texttt{CaKindex}^2 + a_5 \cdot \texttt{sklcomp\_1}^2 \quad (19)$$

$$[\text{Fe/H}] = a_1 + a_2 \cdot \texttt{CaKindex} + a_3 \cdot \texttt{balmsum} + a_4 \cdot \texttt{CaKindex}^2 + a_5 \cdot \texttt{balmsum}^2. \quad (20)$$

We found that the models (16), (19) lead to slightly better results than their alternatives (17), (19), so that we use `sklcomp_1` and `CaKindex` for determining $T_{\rm eff}$ and [Fe/H]. The fit coefficients vary slightly with S/N; thus for each spectrum the appropriate set of coefficients has to be used.

We tested the accuracy of our method by applying it to 6 sets of 165 000 spectra, at $S/N = 5, 10, 15, 20, 25, 30$. Because the parameters of our models have been derived by using these spectra indirectly, it is anticipated that we *underestimate* the errors in this investigation. The results are shown in Fig. 25. For $S/N > 15$, the uncertainties are $\sigma_{T_{\rm eff}} < 130$ K, $\sigma_{\log g} < 0.48$ dex and $\sigma_{[\text{Fe/H}]} < 0.47$. The errors increase sharply at $S/N < 10$, which reinforces our decision to exclude such spectra from the search for metal-poor stars.

As an independent test sample we used 460 stars from the HK survey present on HES plates, with available [Fe/H] estimate, not saturated in the HES, and in the $B-V$ range covered by our model atmospheres, i.e. $0.29 < B-V < 0.70$. The metallicities were scaled to the HES abundance scale using Eq. (24). The standard deviation of the measurements directly in the HES spectra from the moderate resolution spectroscopy results is 0.85 dex. This is 0.38 dex, or by a factor 1.81, higher than expected for the relatively bright stars from the HK survey used as test objects: The average S/N of that sample is ~ 25, which led to $\sigma_{[\text{Fe/H}]} = 0.47$ in the sample of simulated spectra. The lower accuracy is most likely due to the discontinuity effect discussed above.

There is also evidence for a systematic deviation between the two sets of [Fe/H] measurements: The mean difference between is -0.28 dex; i.e., the [Fe/H] estimates directly from HES spectra are too low. Moreover, there is a systematic trend of the [Fe/H] deviations with [Fe/H] itself; i.e., a too low [Fe/H] is assigned to spectra of "metal-rich" objects, and a too high [Fe/H] to spectra of metal-poor objects (see Fig. 26). The former results in contamination of metal-poor star samples selected with this method, and the latter in incompleteness. This method is thus expected to be of restricted usefulness for the selection of metal-poor stars.

4.3.4 Visual Inspection

The final step of the selection is visual inspection of the automatically selected spectra at the computer screen. This step is done for *all* selections described above. Visual inspection is necessary for identification of plate artifacts (e.g. scratches or emulsion flaws), and for rejection of obviously misclassified spectra, i.e. spectra which clearly show a Ca K line. Misclassifications like that happen due to equivalent width measurement errors. The remaining candidates are divided into three classes according to the appearance of the Ca K line region: "class a" candidates show clearly no line; in spectra of "class b"

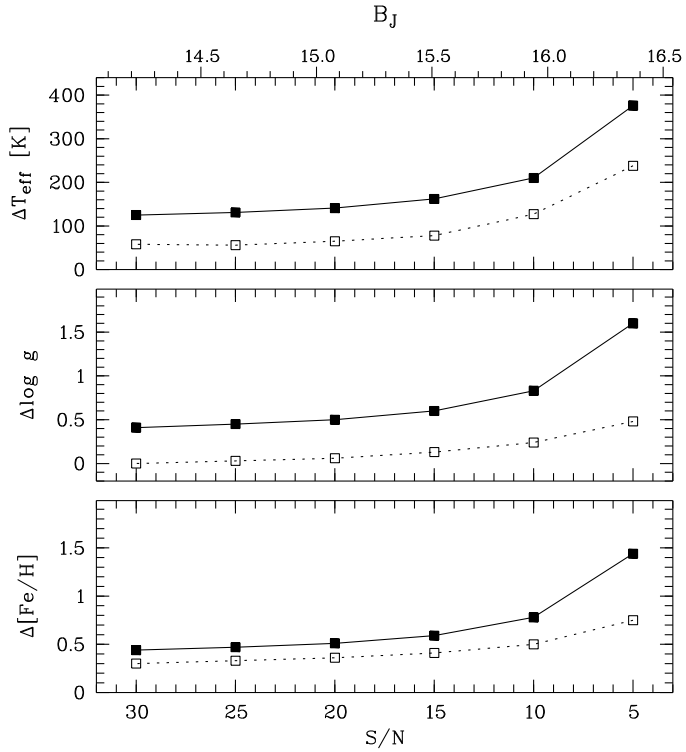

Figure 25: Accuracy of HES feature calibration method for determining stellar parameters directly from HES spectra in dependence of S/N (solid line), compared to accuracy achieved with automatic classification (dotted line). corresponding B_J derived from Eq. (5).

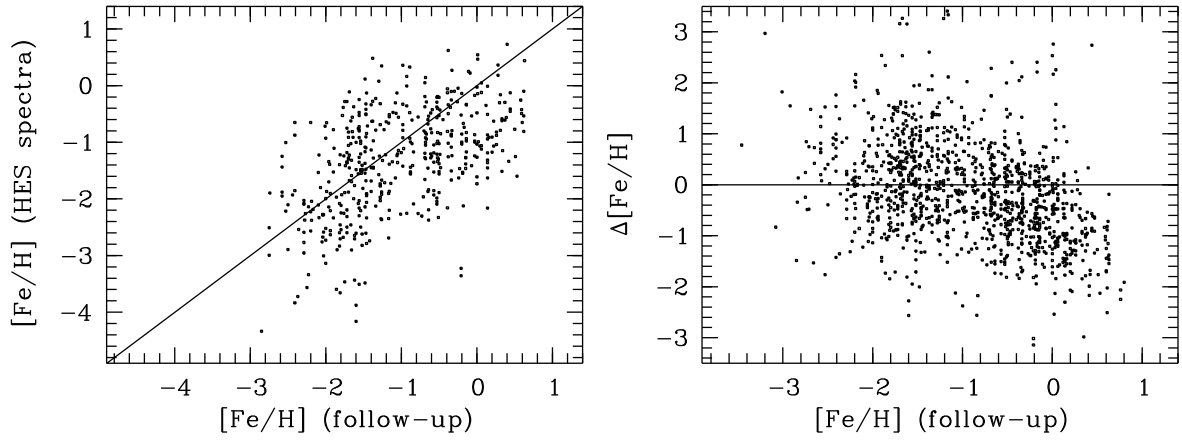

Figure 26: Comparison of [Fe/H] derived from HES spectra with the feature calibration method versus [Fe/H] from moderate resolution follow-up spectroscopy of HK survey stars. [Fe/H] was scaled to the HES abundance scale.

candidates it is unclear if they have a line, and "class c" candidates *do* show a Ca K line, but however, a weak one. Typically, only 10 % of the candidates belong to class a or b, 40 % belong to class c, 25 % are misclassifications, and further 25 % are disturbed spectra.

4.4 Spectroscopic Follow-up techniques

As we have seen in Sect. 4.3, stellar parameters can be derived from HES spectra (and objective prism spectra in general) only with limited accuracy. Therefore, the HES, and all other objective prism surveys, can only provide *candidate* identifications. Because one does not want to spend significant amounts of large telescope time for obtaining high-resolution, high-S/N spectra of uninteresting stars, spectroscopic follow-up observations of such candidates has to be done with great care.

4.4.1 The Ca K-index and ACF Methods

For candidate low-metallicity stars in the HK survey, medium resolution (1–2 Å) spectroscopy and broadband *BV* photometry are used to obtain metallicity estimates using two separate techniques. The first technique relies on the assumption that the strength of the Ca K line tracks the overall stellar [Fe/H], an assumption which is particularly good for stars with [Fe/H] ≤ -1.5. The second is based on an Auto-Correlation Function (ACF, originally described by Ratnatunga & Freeman 1989) of a stellar spectrum. The ACF method is particularly good for stars with [Fe/H] > -1.5, where the Ca K line begins to saturate with increasing metal abundance. Beers et al. (1999) discuss this calibration, and demonstrate, based on comparisons with some 550 stars with external high-resolution abundance estimates, that these approaches used in combination yield abundance determinations with small scatter (on the order of 0.15–0.20 dex) over the entire range of stellar abundances we expect to find in the Galaxy ($-4.0 \leq [\mathrm{Fe/H}] \leq 0.0$).

4.4.2 The "All in One Shot"-Technique

Due to limited telescope time available for follow-up observations, it would be desirable to obtain estimates of stellar parameters, e.g., [Fe/H], T_{eff}, and $\log g$, purely spectroscopically, *without* the need for additional photometry. The first approach attempted with the HES follow-up made use of comparisons with synthetic spectra. However, our experience was that the choice to employ the Mg I b lines as gravity indicators leads to a number of difficulties. For example, satisfactory results required high S/N (> 50) spectra, which are very time consuming to obtain for the fainter stars. Furthermore, at [Fe/H]$\lesssim -2.5$ and turnoff temperatures, Mg I b is so weak that it is not sensitive to gravity anymore. Finally, the comparison of follow-up spectra with synthetic spectra has to be done manually at the computer screen, which is a time sink as well.

As an alternative, the "all in one shot"-technique described below was developed. It is fast, since for each star a single spectrum with $S/N \sim 30$ at Ca K is all that is required, and data analysis can be done fully automatically.

Following the idea of Norris & Freeman (1979), we obtain Strömgren *ubv* directly from the slit spectra by multiplication with filter response curves and integration over the appropriate wavelength range (see Fig. 27). Spectrophotometry of each candidate is obtained by using a wide slit ($\gtrsim 3\times$ seeing disc) rotated to the parallactic angle, to avoid atmospheric slit losses. When using EMMI at the 3.5 m ESO NTT, the spectral coverage required for obtaining Strömgren c_1 coefficients from the spectra (3200 Å $< \lambda <$ 4900 Å) limits the maximum possible dispersion to 1.8 Å per pixel (grating #4), since in the blue arm of EMMI a 1 k CCD is the only available choice. The pixel size is $0\farcs37$, so that at

seeing $< 1\farcs2$, a spectral resolution of < 6 Å results. Exposure times for obtaining $S/N > 30$ at Ca K are 5 min for stars of $B < 17.0$. In the case where stars exhibit a very weak Ca K line, as recognized from online-reduced spectra, an additional, longer, exposure with narrow ($1\farcs0$) slit is obtained. The average total exposure time per object is typically 10 min, which makes it possible to observe ~ 30 metal-poor candidates per night.

The spectra are shifted into the rest frame by cross-correlation with a model spectrum of similar stellar parameters, and applying the appropriate radial velocity correction. Note that the radial velocities derived are not useful measurements in themselves, since the precise position of the object in the (wide) slit is not known. Therefore, zero-point offsets in wavelength can occur.

Three features are used for determination of the stellar parameters [Fe/H], $T_{\rm eff}$, and $\log g$: the Strömgren coefficient c_1, the Hδ index HP2, and the Ca K index KP (for a definition see Beers et al. 1999). The internal accuracy achieved for spectrophotometric c_1 is $\sigma_{c_1} = 0.022$ mag, which compares favorably with errors from photoelectrically measured indices.

Stellar parameters are derived by using the following set of equations:

$$T_{\rm eff} = a_{11} + a_{12} \cdot c_1 + a_{13} \cdot {\rm HP2} \quad (21)$$

$$\log g = a_{21} + a_{22} \cdot c_1 + a_{23} \cdot {\rm HP2} \quad (22)$$

$$[{\rm Fe/H}] = a_{31} + a_{32} \cdot {\rm HP2} + a_{33} \cdot {\rm KP} \quad (23)$$

The coefficients a_{ij} have been determined from least squares fits to the dense grid of model spectra already described above, i.e.

$$\begin{aligned} T_{\rm eff} &= 5600(200)6800\,{\rm K} \\ \log g &= 2.2(0.8)4.6 \\ [{\rm Fe/H}] &= -0.3, -0.9, -1.5(0.3) - 3.6. \end{aligned}$$

Using equations (21)–(23), it was possible to reproduce the stellar parameters of the model spectrum grid with the following accuracy:

$$\begin{aligned} \sigma_{T_{\rm eff}} &= 24\,{\rm K} \\ \sigma_{\log g} &= 0.21 \\ \sigma_{[{\rm Fe/H}]} &= 0.16. \end{aligned}$$

Note that these are *internal* errors for *noise-free* spectra. Unfortunately, due to lack of an independent test sample, it is not yet possible to estimate the *real* accuracy of this approach. However, experience with spectrum synthesis has shown that at the spectral resolution used in the HES follow-up, errors in $\log g$ and [Fe/H] are typically twice as high as the numbers above, and errors in $T_{\rm eff}$ are typically < 200 K.

4.4.3 Neuronal Network Techniques

At the University of Texas in Austin, a group around T. von Hippel is currently exploring the use of Artifical Neuronal Networks (ANNs) for determination of stellar parameters $T_{\rm eff}$, $\log g$ and [Fe/H] from moderate resolution spectra, taken with a narrow slit, so that radial velocities could be obtained simultaneously (see Qu et al. 1998; Snider et al. 2000).

However, looking closely to Snider et al. (2000) reveals that the classification accuracy claimed, i.e. $\sigma_{T_{\rm eff}} = 3\%$ (corresponding to 135–189 K), $\sigma_{\log g} = 0.41$ dex and $\sigma_{[{\rm Fe/H}]} = 0.22$ dex, is doubtful. This

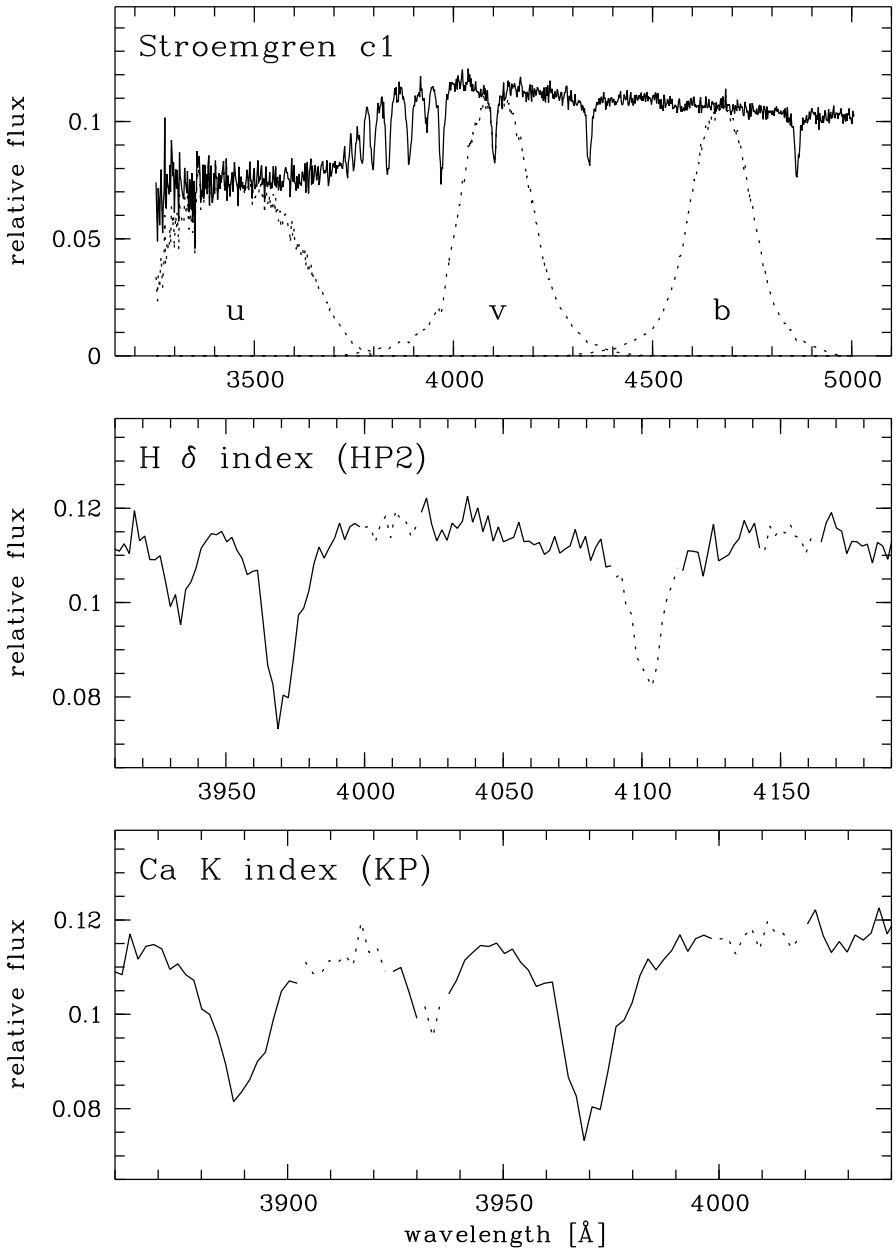

Figure 27: Determination of c_1, HP2, and KP from photometric, moderate resolution ($\sim$ 5 Å) spectra obtained with EMMI attached to the 3.5 m ESO NTT. Dashed lines in the lower two panels indicate continuum and line passbands used for the computation of HP2 and KP, respectively.

is due to the following reasons. In their $T_{\rm eff}$–$\log g$ diagram (also known as "Kiel diagram"), subgiants (SG) and horizontal branch (HB) stars seem to be missing (see Fig. 28). One can see a few points above the main sequence, but one would expect them to be located a bit higher, and there should be more of them, especially close to the turnoff. It is expected that there are very few HB stars above ~ 6000 K, because of the RR Lyrae gap, but one expects a lot more *red* HB stars to be present. This means that either HB stars and SGs have been *excluded* from the learning and test samples, or there is something wrong with the gravity determination.

In the first case, Snider et al. (2000) would underestimate the error of their method in [Fe/H], since there is a degeneracy between high gravity, low metallicity stars and low gravity, high metallicity stars. That is, at the same temperature, a star with e.g. [Fe/H] $= -2.0$ and $\log g = 2.0$ has a Ca K line (used as metallicity indicator) as weak as a [Fe/H] $= -3.0$ and $\log g = 4.8$ star would have.

The accuracy of the $\log g$ determination would be also underestimated as compared to "real life" (that is, as compared to a sample which occupies the Kiel diagram diagram as indicated above), if HB stars and SGs would have been excluded. By just saying that every star at $T_{\rm eff} < 5000$ K has $\log g = 2.5$, and every star at $T_{\rm eff} > 5000$ K has $\log g = 4.5$, one would arrive at an average error for $\log g$ which is probably not far away from 0.41 dex, since the numerous dwarfs, having an almost "flat" distribution in the Kiel diagram, dominate the average error.

If HB stars and subgiants have *not* been excluded, and there is an error in the gravity determination, one can not trust neither the claimed $\log g$ accuracy, nor the [Fe/H] accuracy; the latter being the case again because of the confusion between between high gravity, low metallicity stars and low gravity, high metallicity stars.

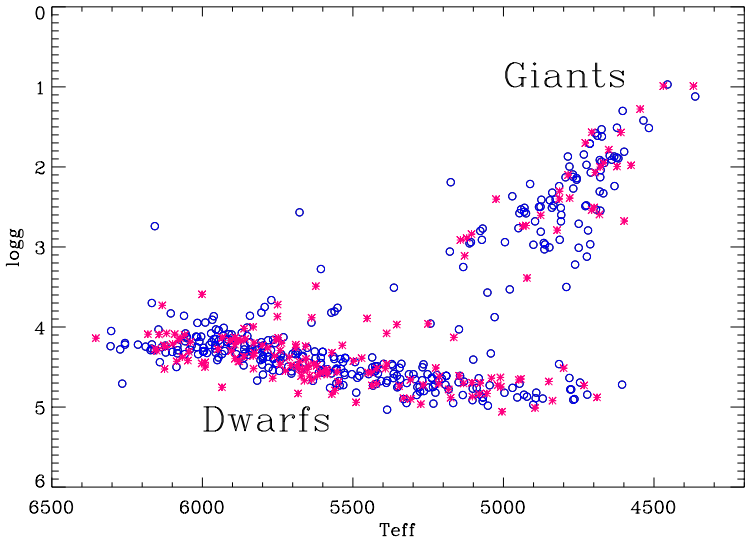

Figure 28: HRD of training and test set of Snider et al. (2000) (their Fig. 2).

A drawback common to all ANN approaches is also that it is very difficult, if possible at all, to understand *how* the classification results were obtained. In case of the determination of stellar parameters from moderate resolution spectra, it would be very interesting to know how the ANN of Snider et al. (2000) carries out the classification in $\log g$, and to learn about the physical reasons behind this. In this way, also any "fake" indicators used in the classification process, like e.g. effective temperature as gravity indicator, as described above, could be identified.

4.5 Effective Yields

As emphasized pointed out by Beers (2000*b*), the *effective yield* (EY) of a detection method is one of the most important properties of a survey for metal-poor stars. EY is defined as follows:

$$\mathrm{EY}_x := \frac{N_{\mathrm{stars\ with\ [Fe/H]} < x}}{N_{\mathrm{stars,\ observed}}}.$$

When EYs for different surveys are compared, it is crucial to make sure that the comparison is done on the same abundance scale. In case of the HK survey and the HES, it was found that metallicities derived from the first-pass analysis of the HES follow-up spectroscopy are ~ 0.5 dex *higher* on average, than obtained from the Beers et al. (1999) re-calibration. That is,

$$[\mathrm{Fe/H}]_{\mathrm{HK}} = [\mathrm{Fe/H}]_{\mathrm{HES}} - 0.5. \tag{24}$$

This offset of the scales is primarily due to the different temperature scales adopted in the two methods. In the HK survey, effective temperatures are (implicitly) derived from *BV* photometry, whereas in the HES, Balmer lines are used. The abundance scale previously employed in the HK survey, e.g. in Beers et al. (1992), is known to be an *additional* 0.2 dex lower for the lowest metallicity stars (see Beers et al. 2000*a*).

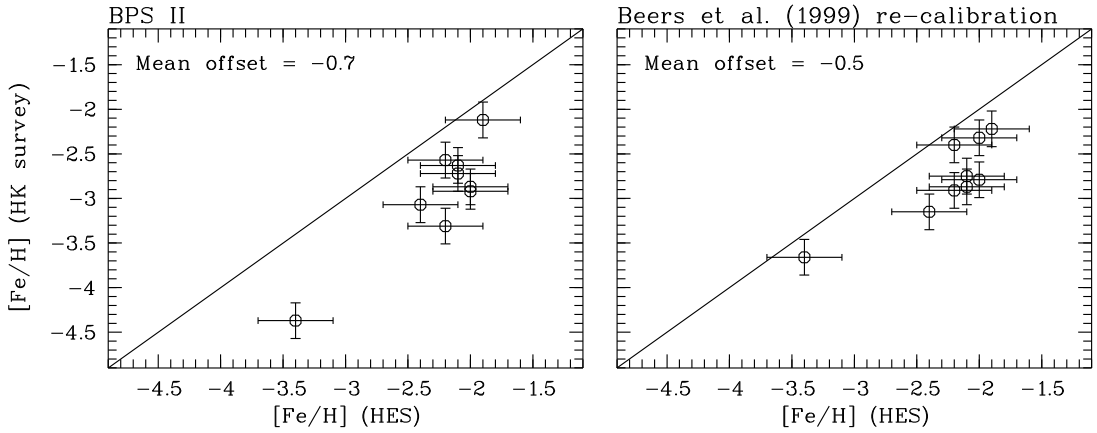

Figure 29: Comparison of HES and HK survey abundance scales. Error bars are 0.2 dex for the HK survey values, and 0.3 dex for HES values.

Thus far, only nine stars have been analyzed with *both* follow-up techniques (see Fig. 29), and there is especially a paucity of comparison objects at $[\mathrm{Fe/H}]_{\mathrm{HES}} < -2.5$. However, the derived trend is consistent for all data points. Only turnoff stars have been used in the comparison; therefore, it can not be excluded that the abundance difference is less (or even more) pronounced for cooler stars.

For this discussion, we restrict our EY comparison to turnoff stars in the color range $0.3 < B-V < 0.5$, and carry out the comparison after an offset of 0.5 dex has been subtracted from the HES metallicities.

In order to explore what the *highest possible* EY in the HES is, we observed a sample of 56 HES metal-poor candidates with EMMI at the ESO NTT. The stars were selected by automatic classification, by using a set of 8 spectral features. These were selected by hand, because at that time the search for the best feature combinations was not yet completed.

Survey/selection method	$EY_{-2.0}$	$EY_{-2.5}$
HK survey/without $B-V$ pre-selection	11 %	4 %
HK survey/with $B-V$ pre-selection	32 %	11 %
HES/automatic classification	80 %	27 %

Table 9: Comparison of effective yields (EY) of metal-poor turnoff stars of the HK survey and the HES. [Fe/H] is on the re-calibrated HK survey scale of Beers et al. (1999).

The automatic classification programs were fed only with a subset of all spectra present on each HES plate. As already mentioned, only spectra with $S/N > 10$ and $B \gtrsim 14$ are considered. Moreover, spectra outside of the range $0.3 < B-V < 0.5$ are excluded, where $B-V$ is known to ± 0.1 mag from the calibration of `x_hpp2`.

Below we summarize the selection criteria for metal-poor stars in the HES for the selection by automatic classification. Pre-selection of spectra to which automatic classification procedures are applied is done by criteria (1)–(3); (4) and (5) use the results of automatic classification, and (6) is a rejection criterion corresponding to a χ^2 test at a 3σ level.

(1) $0.3 < B-V < 0.5$

(2) $(S/N)_{\rm HES} > 10 \Longleftrightarrow B \lesssim 16.5$

(3) Photographic density D below saturation threshold

(4) $\log g \geq 3.8$

(5) $[\mathrm{Fe/H}] \leq -2.7$

(6) $a.i. < 0.99$.

Only candidates assigned classes a or b in the visual inspection have been observed. EY of stars at [Fe/H] < -2.0 for this sample is 80 % (see Tab. 9)! This has to be compared with 11 % or 32 % in the HK survey, depending on whether a pre-selection based on $B-V$ color has been made or not, respectively.

4.6 Discussion and Conclusions

Selection of metal-poor candidates at the main-sequence turnoff in the HES by automatic classification is $\sim 3\times/\sim 7\times$ more efficient as compared to visual inspection in the HK survey with/without pre-selection by *BV* photometry. This is very remarkable considering the fact that the spectral resolution of the HES is $2\times$ *lower* than in the HK survey. Reasons for the higher efficiency are the larger spectral coverage of the HES, better quality of the HES spectra, and the automated, quantitative selection, which is presumably more precise than the selection by eye. Moreover, we have intentionally observed class a and b candidates only, because we wanted to explore what the *maximum possible* efficiency is. Simulations we have carried out indicate that, in exchange for a high EY of truly metal-poor stars, one has to sacrifice completeness of the candidate sample on the order of 50 %. Thus, the EY of a selection aimed at compiling a *complete* sample of metal-poor stars by means of including class c candidates, and also candidates from complementary selection methods (e.g. the feature calibration method), will be proportionately lower.

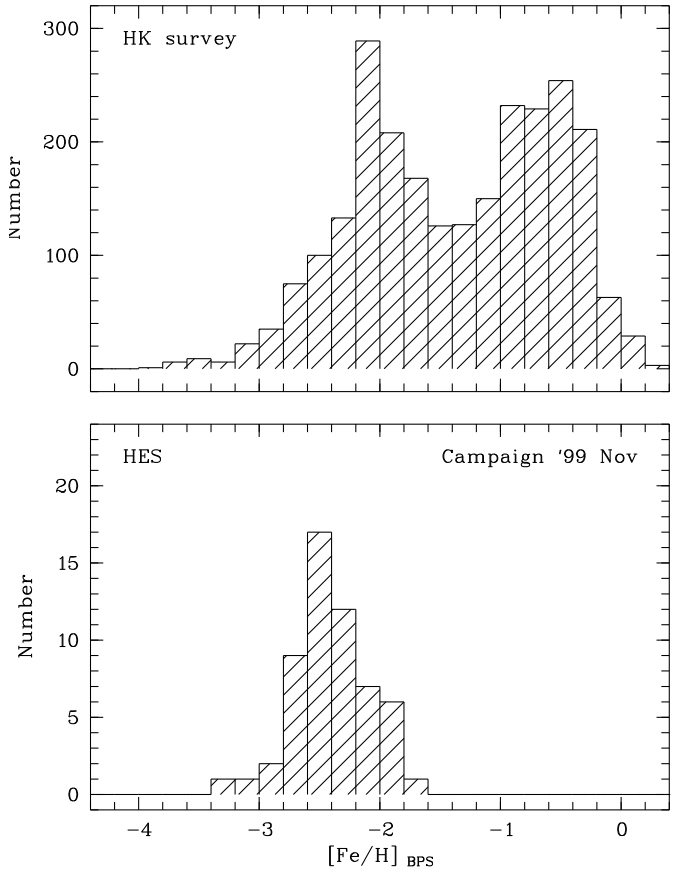

Figure 30: Metallicity distribution function of stars in the color range $0.3 < B-V < 0.5$ from the HK survey (upper panel), and of a sample of 56 stars selected by automatic classification in the HES. Note the prominent lack of high metallicity ([Fe/H] > -1.5) stars in the HES sample compared to the HK survey sample.

It is possible to derive rough stellar parameters for stars in the range $5200\,\mathrm{K} < T_{\mathrm{eff}} < 6800\,\mathrm{K}$ directly from HES spectra by either automatic classification, or the calibrated feature approach. Experiments are carried out to do the same for digitized HK survey spectra, by using ANNs (Rhee et al. 1999). However, since only a small spectral range is covered by the HK survey, so that much less information, and in particular no colour information, is included in those spectra, it is even more challenging to do this in the HK survey.

The follow-up technique used in the HK survey results in determinations of [Fe/H] precise to ± 0.2 dex; the accuracy of the HES technique remains to be evaluated. The advantage of the "all in one shot"-technique used in the HES is that no photometry is needed in addition to moderate resolution spectra. However, a drawback is that no useful radial velocities can be measured from spectra obtained with the wide slit, since the object position within the slit is not precisely known, so that unknown zero-point offsets in wavelength occur.

In follow-up campaigns carried out so far, 90 metal-poor stars were discovered; 11 are unevolved stars at $[\mathrm{Fe/H}]_{\mathrm{HK}} \leq -3.0$ (see Tab. 24 in Appendix A). In the HK survey, 37 stars with $[\mathrm{Fe/H}]_{\mathrm{HK}} \leq -3.0$, and $0.3 < (B-V)_0 < 0.5$ were found (Beers 2000, priv. comm.). We thus increased the number of unevolved, extremely metal-poor stars already noticeably.

When compiling target lists for high-resolution observations, combining stars from different surveys, it is important to take into account their different abundance scales. An offset of 0.5 dex has to be subtracted from [Fe/H] estimates obtained from the HES follow-up, when they are compared with [Fe/H] values derived from the HK survey.

Since the limiting magnitude for metal-poor stars in the HES is ~ 17.0, and "saturated" objects are excluded from the selection procedure, the HES provides mainly fainter candidates, in the magnitude range $14.0 < B < 17.0$, whereas the HK survey is able to provide bright candidates in the range $11.0 < B < 15.5$.

The HES is ~ 1.5 mag deeper than the HK survey. Therefore, the former can increase the total survey volume for metal-poor stars by a factor of 8, taking into account common areas and the magnitude ranges of both surveys. We estimate that the total number of stars at $[\mathrm{Fe/H}]_{\mathrm{HK}} < -3.0$ known today, ~ 100, can be increased to ~ 400 by the HES, provided that follow-up observations can be obtained for all candidates. Extension of the procedures described above for the inclusion of cooler stars, and complementation of the selection by automatic classification with alternative procedures such as the Ca K index method, could easily increase the number of stars with $[\mathrm{Fe/H}]_{\mathrm{HK}} < -3.0$ to even higher numbers.

4.7 Outlook

4.7.1 Moderate-Resolution Spectroscopic Follow-Up

The bottleneck in searching extremely metal-poor stars are spectroscopic follow-up observations, because even in objective prism surveys with relatively high spectral resolution, like the HK survey, or the HES, it becomes difficult to detect the strongest metal line, i.e. Ca K, at $[\mathrm{Fe/H}]_{\mathrm{HK}} \lesssim -2.0$. Therefore, one is basically "blind" below this metallicity, i.e., one can not distinguish between e.g. a $[\mathrm{Fe/H}]_{\mathrm{HK}} = -2.5$ star and a star of $[\mathrm{Fe/H}]_{\mathrm{HK}} < -3.0$. Unfortunately, the low metallicity tail of the halo metallicity distribution function (MDF) peaks around $[\mathrm{Fe/H}]_{\mathrm{HK}} = -2.2$ (see Fig. 30), so that one has to "fight" against stars of moderately low metal abundance when searching for extremely metal-poor stars. From Tab. 1 in Beers (1999) it can be seen that even if it is possible to exclude all stars of $[\mathrm{Fe/H}]_{\mathrm{HK}} > -2.0$ from the candidate sample, which is already quite challenging, one has to observe ~ 10 stars for finding a star of $[\mathrm{Fe/H}]_{\mathrm{HK}} < -3.0$, and for each star of $[\mathrm{Fe/H}]_{\mathrm{HK}} < -3.5$, one has to observe ~ 60 stars.

For these reasons, it is impossible to make a considerable progress in finding extremely metal-poor stars by using the capacities of a single observatory, like ESO. Therefore, we have established a number of international collaborations by which we gain access to non-ESO telescopes. The telescopes involved are listed below.

ESO Telescopes Due to continued technical problems with EMMI, we will use EFOSC2 attached to the 3.6 m telescope in the future only. Now that we were able to prove that our selection methods work, we received for the first time as many nights as we have requested, i.e. 5 nights per semester. Since our program was proposed as long term project, we expect that we will continue to receive a similar amount of observing time over the next years. Experience at the NTT has shown that it is possible to observe ~ 30 candidates per night in average weather conditions. Therefore, we expect to get spectra of up to ~ 300 candidates per year at ESO.

UK Schmidt/6dF The multi-object spectrograph 6dF (Watson 1998), mounted at the UK Schmidt telescope, is scheduled to come into operation in November 2000. With 6dF it is possible to observe up to 150 targets in a field of view of $6^\circ \times 6^\circ$. At the spectral resolution required for metal-poor star follow-up, objects down to $B \approx 16.5$ can be observed. This would lead to two sets of 4×1 h exposures per night. At $B > 16.5$, the surface density of metal-poor stars from the HES and HK survey combined is ~ 30 per 6dF field (the remaining fibers could be filled with other HES targets, e.g. candidate FHB/A stars, and candidate white dwarfs). It is thus possible to observe ~ 60 metal-poor candidates per night, which is twice as much as is possible with single slit spectroscopy at a 4 m class telescope. In collaboration with M. Bessell (ANU), we will submit a first proposal in summer 2000. Should it be possible to get ~ 2 weeks of observing time per year, about 800 candidates per year could be observed.

2.3 m MSSSO Telescope Again in collaboration with M. Bessell, and J. Norris (ANU) we will ask for observing time at the 2.3 m MSSSO telescope in the period August–October 2000. At that time, 6dF will not yet be in operation. It is probably neither recommended, nor promising to continue submitting proposals for the 2.3 m *after* 6dF is available, so that we will use this telescope only temporarily. Two nights in May have already been granted to us.

CTIO/KPNO 4 m The author is Co-I of a "NOAO Survey Program" aiming at follow-up of metal-poor candidates from the HK survey and the HES. In that proposal we asked for 10 nights per year at the CTIO 4 m, and additional 5 nights per year at the KPNO 4 m, over a period of 5 years. Should the proposal be accepted, we would be able to observe some 500 HES targets per year.

CFHT In a collaboration with D. VandenBerg (University of Victoria, Canada) we have access to the CFHT. A first proposal asking for 5 nights in December 2000 is about to be submitted.

Taking into account a time loss of $\sim 1/3$ of due to bad weather or technical problems, we estimate that $\sim 3\,500$ HES candidates will be observed within the next 3 years, which should at least double the number of stars of $[\mathrm{Fe/H}]_{\mathrm{HK}} < -3.0$.

4.7.2 High-Resolution Spectroscopy

VLT/UVES A first proposal asking for observing time in period 65 (April–October 2000) has been *rejected*. A refined proposal will be submitted in the next period.

Two HES metal-poor stars have already been observed with VLT UT2 in the course of UVES science verification. These stars are HE 1303−2708 and HE 1353−2735. The spectra have $R = 45\,000$, and $S/N > 50$ per pixel throughout the whole spectral range covered, which is $\lambda = 5940$–9750 Å. An additional $S/N > 50$ spectrum in the range $\lambda = 4090$-5310 Å has been taken for HE 1353−2735. These spectra are currently being reduced and will be analyzed soon.

Subaru/HDS The instrument group of the High Dispersion Spectrograph (HDS), scheduled to be mounted at the Subaru telescope in February 2000, has ~ 40 nights of test observing time available to them. We (and other people, working in other fields of astronomy) were asked to submit proposals for observations of HES metal-poor stars using this time. We expect to receive first data by mid-2000. These observations are seen as start of a long-term collaboration from both sides.

Keck/HIRES J. Cohen from the California Institute of Technology has access to the Keck telescope and is interested in collaborating on high-resolution spectroscopy of HES metal-poor stars with HIRES. A first proposal for 4 nights in the period August–September 2000 has been submitted.

Acknowledgements

I thank T. Beers for a trustful and close collaboration. I am especially appreciating that he provided me with the result of almost two decades of work, his master list of all HK survey stars that had follow-up spectroscopy and/or photometry. This list is largely unpublished. Tim also smoothed my English in those parts of this sections that have been taken from Christlieb & Beers (2000).

The first paragraph of Sect. 4.2 is an adapted version of a paragraph in Christlieb & Beers (2000) written by T. Beers. The description of the HK survey candidate selection (2nd paragraph on page 37), and Sect. 4.4.1, are from the same source, and were included in original form.

J. Reetz and T. Gehren contributed to the search for metal-poor stars in the HES by providing model atmospheres, SIU (a tool for spectrum analysis), repeated hospitality at their institute, and many discussions.

I thank J. Norris for bringing the idea of deriving Strömgren c_1 from photometric spectra to my attention.

References

Beers, T. C. (1999), Low-Metallicity and Horizontal-Branch Stars in the Halo of the Galaxy, *in* B. Gibson, T. Axelrod & M. Putman, eds, 'The Third Stromlo Symposium: The Galactic Halo', Vol. 165 of *ASP Conf. Ser.*, pp. 202–212.

Beers, T. C. (2000*a*), Observational constraints on the Nature of the first stars – final comments, *in* A. Weiss, T. Abel & V. Hill, eds, 'The First Stars, Proceedings of the second MPA/ESO workshop', Springer, Heidelberg.

Beers, T. C. (2000*b*), Population III by popular demand – progress and previews, *in* A. Weiss, T. Abel & V. Hill, eds, 'The First Stars, Proceedings of the second MPA/ESO workshop', Springer, Heidelberg. astro-ph/9911171.

Beers, T. C., Chiba, M., Yoshii, Y., Platais, I., Hanson, R. B., Fuchs, B. & Rossi, S. (2000*a*), 'Kinematics of Metal-Poor Stars in the Galaxy. II. Proper Motions for a Large Non-Kinematically Selected Sample', AJ, submitted.

Beers, T. C., Preston, G. W. & Shectman, S. A. (1992), 'A search for stars of very low metal abundance. II.', *AJ* **103**(6), 1987–2034.

Beers, T. C., Rossi, S., Norris, J. E., Ryan, S. G. & Shefler, T. (1999), 'Estimation of Stellar Metal Abundance. II. A Recalibration of the Ca II K Technique, and the Autocorrelation Function Method', *AJ* **117**, 981–1009.

Beers, T. C., Suzuki, T. K. & Yoshii, Y. (2000*b*), The Light Elements Be and B as Stellar Chronometers in the Early Galaxy, *in* L. da Silva, M. Spite & J. R. de Medeiros, eds, 'to appear in: IAU Symposium 198: The Light Elements and Their Evolution', ASP Conf. Ser., ASP, San Francisco.

Bond, H. E. (1981), 'Where is population III?', *ApJ* **248**, 606–611.

Cayrel, R. (1996), 'The first generation of stars', *A&A Rev.* **7**, 217–242.

Christlieb, N. & Beers, T. C. (2000), Ongoing Large Surveys for Metal-Poor Stars in the Galactic Halo, *in* M. Takada-Hidai, ed., 'to appear in: 2nd Subaru HDS Workshop', National Astronomical Observatory, Tokyo. astro-ph/0001378.

Cowan, J. J., Pfeiffer, B., Kratz, K.-L., Thielemann, F.-K., Sneden, C., Burles, S., Tytler, D. & Beers, T. (1999), 'R-Process Abundances and Chronometers in Metal-poor Stars', *ApJ* **521**, 194–205.

Fuhrmann, K. (1999), 'The Disk Populations in the [Mg/H]-[Fe/Mg] Plane', *Ap&SS* **265**, 265–268.

Norris, J. E. & Freeman, K. C. (1979), 'The cyanogen distribution of the giants in 47 Tucanae', *ApJ* **230**, L179–L182.

Qu, Y., Snider, S., von Hippel, T., Sneden, C., Lambert, D., Beers, T. & Rossi, S. (1998), 'Neural Network Techniques Applied to Low Resolution Spectra of Halo Stars', *BAAS* **193**, #44.09.

Ratnatunga, K. U. & Freeman, K. C. (1989), 'Field K Giants in the Galactic Halo. II. Improved Abundance and Kinematic Parameters', *ApJ* **339**, 126–148.

Rhee, J., Beers, T. C. & Irwin, M. J. (1999), 'Automatic Identification, Classification, and Abundance Estimation for Metal-Poor Stars in the Galaxy from Objective-Prism Spectroscopy Using a Neural Network Analysis', *BAAS* **31**, 971.

Shigeyama, T. & Tsujimoto, T. (1998), 'Fossil Imprints of the First-Generation Supernova Ejecta in Extremely Metal-deficient Stars', *ApJ* **507**, L135–L139.

Snider, S., Qu, Y., Allende-Prieto, C., von Hippel, T., Beers, T. C., Sneden, C., Lambert, D. L. & Rossi, S. (2000), 'Teff, log g, [Fe/H] Classification of Low-Resolution Stellar Spectra Using Artificial Neural Networks', *in* 11th Cambridge Workshop on Cool Stars, in press (astro-ph/9912404).

Tsujimoto, T., Shigeyama, T. & Yoshii, Y. (2000), 'Probing the Site for r-Process Nucleosynthesis with Abundances of Barium and Magnesium in Extremely Metal-Poor Stars', ApJ Letters, in press (astro-ph/0001220).

Watson, F. (1998), 'Board's green light for 6dF', *AAO Newsletter* (85), 11–12.